Neurocomputing 436 (2021) 126–135

Contents lists available at ScienceDirect

Neurocomputing

journal homepage: www.elsevier.com/locate/neucom

Effects of burst-timing-dependent plasticity on synchronous behaviour in neuronal network

João Antonio Paludo Silveira [a], Paulo Ricardo Protachevicz [b], Ricardo Luiz Viana [a,*], Antonio Marcos Batista [b,c,d]

[a] Department of Physics, Federal University of Paraná, 82590-300 Curitiba, PR, Brazil
[b] Physics Institute, University of São Paulo, 05508-090 São Paulo, SP, Brazil
[c] Department of Mathematics and Statistics, State University of Ponta Grossa, 84030-900 Ponta Grossa, PR, Brazil
[d] Graduate Program in Science – Physics, State University of Ponta Grossa, 84030-900 Ponta Grossa, PR, Brazil

ARTICLE INFO

Article history:
Received 9 July 2020
Revised 12 November 2020
Accepted 8 January 2021
Available online 18 January 2021
Communicated by Zidong Wang

Keywords:
Plasticity
Rulkov neurons
Synchronisation

ABSTRACT

Brain plasticity or neuroplasticity refers to the ability of the nervous system to reorganise itself in response to stimuli. For instance, sensory and motor stimulation, memory formation, and learning depend on brain plasticity. Neuronal synchronisation can be enhanced or suppressed by the plasticity. Synchronisation is related to many functions in the brain, as well as to some brain disorders. One possible plasticity rule is the burst-timing-dependent plasticity (BTDP), that induces synaptic alteration according to the timing of neuronal bursts. In this work, we build a network of coupled Rulkov maps where the excitatory connections are randomly distributed. We consider the BTDP to study its effects on the synchronous neuronal activities. In our simulations, we observe that depending on the initial synaptic weights, the whole network or part of it can have its neuronal synchronisation improved. This increase can be reached by two different mechanisms, the initial burst synchronisation and random statistical coincidence. A mix of these two mechanism is also found in the network. BTDP can induce the formation of desynchronised and synchronised clusters that operate in different frequencies, but only if the noise level is low. Our results show possible mechanisms of cluster formation in burst neuronal networks. We also consider the BTDP rule on a small-world network and show that, depending on the initial connection strength, the network can exhibit local or non-local properties.

1. Introduction

The brain is an organ with one of the most complex structure in the human body [1]. It is constituted by billions of neurons that are connected to each other by means of a large number of synapses [2]. Through neurons, information can be transmitted between brain regions by electrochemical signals [3]. The information is relayed through electrical and chemical synapses by different mechanisms [4].

The brain can modify its organisation and function throughout life. This ability is known as neuroplasticity or brain plasticity and can occur in response to stimuli or injury [5]. The existence of changes in the brain functions was proposed by James [6] in 1890. In the late 1800s, Cajal [7] used the term plasticity to describe brain adaptation due to the environment. Alterations in neuronal pathways were observed in experiments performed in 1923 by Lashley [8]. Hebb [9] in 1949 postulated that the synapse between two neurons is potentiated when they are active at the same time. Two decades after the Hebb's rule, experimental results about the potentiation were found in the rabbit hippocampus [10].

Mathematical models of networks have been considered to mimic effects of plasticity in neuronal activities [11]. Popovych et al. [12] studied the noise dependency of synchronous behaviour in a neuronal network model with spike-timing-dependent plasticity (STDP). Borges et al. [13–15] reported that STDP can induce non trivial topology in the brain. Another type of neuroplasticity is the burst-timing-dependent plasticity (BTDP) [16], that induces synaptic alteration according to the timing of bursts. Recently, Wang et al. [18] found the coexistence of coherent and incoherent dynamics, known as chimera states, in an adaptive neuronal network with BTDP.

Plasticity influences synchronous behaviour and its transition in neuronal networks [19]. Neuronal synchronisation has been observed in the brain during different tasks [20]. Jiang et al. [21] showed results in which the synchronisation increases in the left

* Corresponding author.
E-mail address: viana@fisica.ufpr.br (R.L. Viana).

https://doi.org/10.1016/j.neucom.2021.01.044
0925-2312/

inferior frontal cortex during a face-to-face dialogue. Strong and weak synchrony have been detected in neurological disorders [22], such as Parkinson's [23] and Alzheimer's diseases [24]. Epilepsy has been considered as a disorder characterised by seizures and is related to synchronised neuronal activities [25].

We build a network composed of coupled Rulkov maps [26]. The model proposed by Rulkov [27] in 2001 is a two dimensional iterated map that has been used to describe the dynamics of bursting activity of biological neurons. We consider two types of network structure. In the first, the neurons are randomly connected according to the Erdös-Rényi model [28], where excitatory chemical synapses are distributed by means of a connection probability. The second kind is a small-world network constructed with the Watts-Strogatz method [30]. Small-world networks are known to minimize the wiring cost, and many small-world properties have been found in the brain [31]. We consider a burst-timing-dependent plasticity (BTDP) rule that was introduced by Butts et al. [16]. In this work, we focus on the effects of the BTDP in the neuronal synchronisation. The BTDP changes the synaptic weight, and as a consequence it can induce or reduce synchronous behaviour. We observe increase of synchronisation due to plasticity for initially synchronous and de-synchronous states. We identify two different mechanisms that are associated with the potentiation of the synaptic weights. We also show the formation of clusters with different frequencies is possible during the synchronisation improvement. Therefore, BTDP plays an important role in neuronal synchronisation.

This paper is organised as follows: In Section 2 we introduce the neuronal network model with BTDP. In Section 3, we discuss our results about the plasticity. In the last Section, we draw our conclusions.

2. Neuronal network model

The neurons are modelled by the Rulkov model, given by

$$x_{i,t+1} = \frac{\alpha_i}{1+x_{i,t}^2} + y_{i,t} + I_{i,t} + \epsilon\xi_{i,t}, \tag{1a}$$

$$y_{i,t+1} = y_{i,t} - \sigma x_{i,t} - \beta. \tag{1b}$$

$x_{i,t}$ represents the membrane potential of the ith neuron ($i = 1, 2, \ldots, N$) at the discrete time t and y_i is the slow time-scale variable which generates the bursting behaviour on the variable x_i. The behaviour of the x and y variables of a single uncoupled neuron is depicted in Fig. 1. In our simulations, we use $\sigma = 0.0009$ and $\beta = 0.0011$. The parameter α_i is randomly distributed in the interval $[4.1, 4.4]$ with uniform probability. The parameter α_i controls the neuron's mean natural bursting frequency f_0 (the mean burst frequency it exhibits when uncoupled) and, in the used interval, there is an approximately linear relationship, that is given by

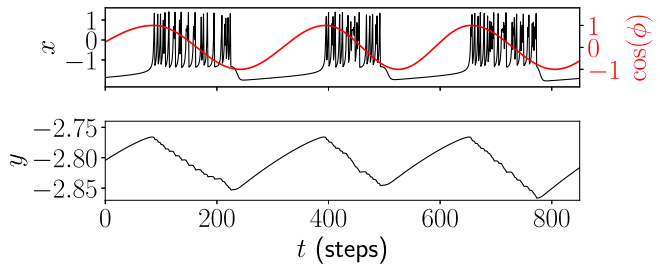

Fig. 1. Time series of the x and y variables of an uncoupled Rulkov map neuron with $\alpha = 4.2, \sigma = 0.0009$, and $\beta = 0.0011$. The x variable exhibits bursting behaviour and is interpreted as the neuron's membrane potential. The cosine of the neuron's phase is plotted in red. (For interpretation of the references to colour in this figure legend, the reader is referred to the web version of this article.)

$f_0 = 0.01137\alpha - 0.04408$. $\xi_{i,t}$ is a gaussian white noise applied with no correlation with respect to time or the applied neurons. ϵ is the noise amplitude.

We build a network of $N = 1000$ neurons connected to each other by means of excitatory chemical synapses. We represent the synaptic current injected on the neuron i at time t as [29]

$$I_{i,t} = -\frac{1}{\chi}(x_{i,t} - V_s)\sum_{j=1}^{N} A_{ij} W_{ij,t} H(x_{j,t} - \theta), \tag{2}$$

where $H(x)$ is the Heavyside step function, $\theta = 0$ is the spiking threshold of the membrane potential, $V_s = 1$ is the reversal potential, and $\chi = (1/N)\sum_{ij}^{N} A_{ij}$ is the network's mean connectivity that is used for normalization. A_{ij} is an element of the adjacency matrix and assumes the value 1 if a connection from neuron j to neuron i exists, and 0 otherwise. Two connection schemas were used, both directed complex networks. The first is a random network built using the Erdös-Rényi method [28] with connection probability $p = 0.35$. The second is a small-world network built using the Watts-Strogatz algorithm [30] with mean connectivity $k = 4$ and rewiring probability $\beta = 0.2$. Each connection structure will be analysed separately. $W_{ij,t}$ is the synaptic weight of the synapse $j \to i$ at time t. It can be interpreted as a synaptic conductance and controls how strong the connection is. $W_{ij,t}$ can assume values between 0 and $W_{\max}$, and it can change over time following the plasticity rule. For the random network $W_{\max}$ is equal to $W_{\max}^{\mathrm{ER}} = 0.1$, while for the small-world network $W_{\max}^{\mathrm{WS}} = 0.2$. To modify the synaptic weights as the network evolves, we use the burst-timing-dependent plasticity (BTDP) rule [16]. It uses the time difference between the burst-start times (or burst latency) of two connected neurons to determine the synaptic weight change according to the equation

$$\Delta W(\Delta t) = \begin{cases} A_p - \frac{A_p - A_d}{T_s}|\Delta t| & \text{if} \quad |\Delta t| \leqslant T_s \\ A_d & \text{if} \quad |\Delta t| > T_s \end{cases} \tag{3}$$

with $A_p = 0.008, A_d = -0.0032$, and $T_s = 58$. A plot of the BTDP function is shown in Fig. 2. If both neurons burst at similar times, then potentiation occurs, but if the time difference between the burst-start events is large enough, depression occurs. The parame-

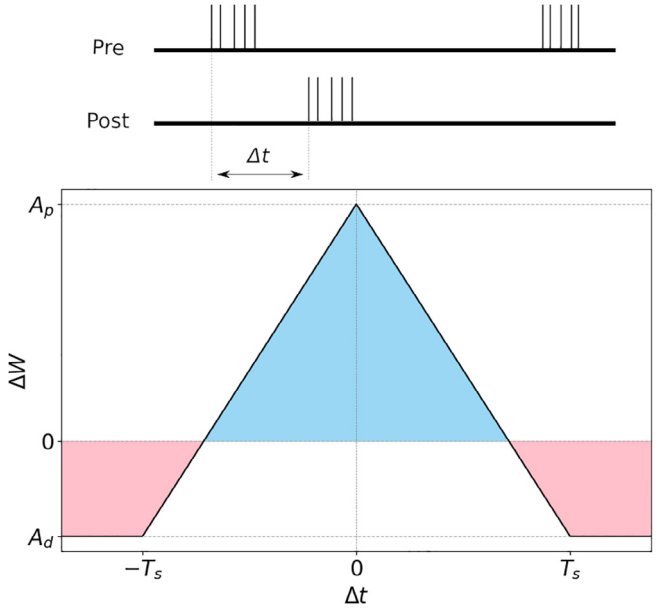

Fig. 2. Change on synaptic weight as a function of the time latency between the burst-start events of two connected neurons. Bursts starting close together cause synapse potentiation, while large burst latency causes depression.

ter values are chosen to keep the ratio $|A_d/A_p| \approx 0.4$ [16], as well as to adapt the time scale of the curve to the discrete time of the Rulkov map.

The change in the synaptic weight is additive and calculated through Eq. 3 with Δt equal to the difference between the current time and the last burst-start time of the neuron's neighbour. By doing this, all synapses are updated twice for burst pair (W_{ij} is updated both when i starts a burst and when j does). To correct this, we change $A_d \to D = A_d/2$ and $A_p \to P = A_p + D$ in the implementation of Eq. 3. This ensures that, after both updates are considered, the effective synaptic weight change reflects the amplitudes A_p and A_d. In addition we limit the values of the synaptic weights in the range $0 \leqslant W_{ij} \leqslant W_{\max}$. If the application of the plasticity rule results in a negative synaptic weight, or one greater than $W_{\max}$, the synaptic weight value is set to the trespassed limit. This is done to avoid that the synapses become inhibitory, as well as to avoid unlimited injection of current, which can destroy the bursting dynamics of the.

The initial conditions are randomly chosen in the interval $x_i = [-2, 2]$ and $y_i = [-4, 0]$. All synapses are initiated with the same synaptic weight W_0. After a transient of $t_{\text{trans}} = 10^4$ steps in which the neurons are active but the plasticity is not computed, the network is let to evolve for 1.5×10^6 steps. During this time interval, the synaptic weights vary according to the plasticity rule, and the network synchronisation level is measured. To analyse the burst synchronisation of the network, we consider the neuron's phase ϕ_i, that is written as

$$\phi_{i,t} = 2\pi\left(k + \frac{t - t_{k,i}}{t_{k+1,i} - t_{k,i}}\right) \qquad t_{k,i} \leqslant t < t_{k+1,i}, \tag{4}$$

where t is the current time, $t_{k,i}$ is the time of the kth burst of the ith neuron, and the first burst is labelled by the index $k = 0$. Fig. 1 displays the evolution of $\cos\phi$ for a Rulkov neuron.

The network synchronisation level is measured by the absolute value of the Kuramoto order parameter [17], defined by

$$R_t = \left|\frac{1}{N}\sum_{i=1}^{N} e^{\mathrm{j}\phi_{i,t}}\right|, \tag{5}$$

where $\mathrm{j} = \sqrt{-1}$ is the imaginary unit. R_t is a real number between 0 and 1, and it assumes its highest value when the network is completely synchronised (all neurons burst at the same time) and 0 when there is no synchronisation in the network. The mean Kuramoto order parameter is calculated as

$$\overline{R} = \frac{1}{t_{\text{fin}} - t_{\text{ini}}}\sum_{t=t_{\text{ini}}}^{t_{\text{fin}}} R_t, \tag{6}$$

where $t_{\text{ini}} = t_{\text{tran}} = 10^4, t_{\text{fin}} = 2 \times 10^4$; and $t_{\text{ini}} = 149 \times 10^4, t_{\text{fin}} = 150 \times 10^4$.

The mean synaptic weight is given by

$$\langle W\rangle = \frac{1}{N_{\text{syn}}}\sum_{i,j=1}^{N} W_{ij}A_{ij}, \tag{7}$$

where $N_{\text{syn}} = \sum_{ij=1}^{N} A_{ij}$ is the total number of synapses in the network.

The mean burst frequency of a neuron is computed as the inverse of the mean inter-burst-interval ($\bar{f}_i = 1/\overline{\text{IBI}}_i$). As done for the order parameter, the mean frequency is calculated at the initial state ($t_{\text{trans}} < t \leqslant t_{\text{trans}} + 10^4$) and at the final state ($149 \times 10^4 < t \leqslant 150 \times 10^4$). These are called as the initial mean frequency $\bar{f}_{i,\text{ini}}$ and the final mean frequency $\bar{f}_{i,\text{fin}}$, respectively. We also consider the neuron's natural mean frequency $f_{i,0}$, which is the frequency that the neuron has when is isolated. This quantity is intrinsic and is obtained using a linear relation with the parameter α.

3. Results

3.1. Random network

Aiming to study the effects of BTDP on the random network, we calculate the mean synaptic weight, mean order parameter, and frequency of the neurons in the asymptotic state. In Fig. 3(a), we show the network's average synaptic weight $\langle W\rangle$ of the final state as a function of the initial synaptic weight W_0 in the case of no noise ($\epsilon = 0$). The initial synaptic weight is indicated by the grey diagonal line. In our simulations, all initial synaptic weights are considered equal to W_0. We observe that in the asymptotic states, all synapses end up with a synaptic weight very close to either 0 or $W^{\text{ER}}_{\max}$. This polarisation of synaptic weights happens regardless of their initial values (W_0), although the fraction of synapses at each extreme varies. Because of this, $\langle W\rangle/W^{\text{ER}}_{\max}$ is the proportion of synapses with maximum weight.

We observe that for almost all W_0, the final state has a larger mean synaptic weight value than the initial state, and as a consequence, the potentiation is overall favoured over depression. However, the increase of the mean synaptic weight depends on the initial weight value. For $W_0 \leqslant 0.45W^{\text{ER}}_{\max}$ and $W_0 \geqslant 0.55W^{\text{ER}}_{\max}$, the curve in Fig. 3 looks very smooth. These two curves suggest that there are two distinct regimes with some transition state connecting them. The connection region can be approximately identified in the interval $0.45W^{\text{ER}}_{\max} < W_0 < 0.55W^{\text{ER}}_{\max}$. The potentiation that

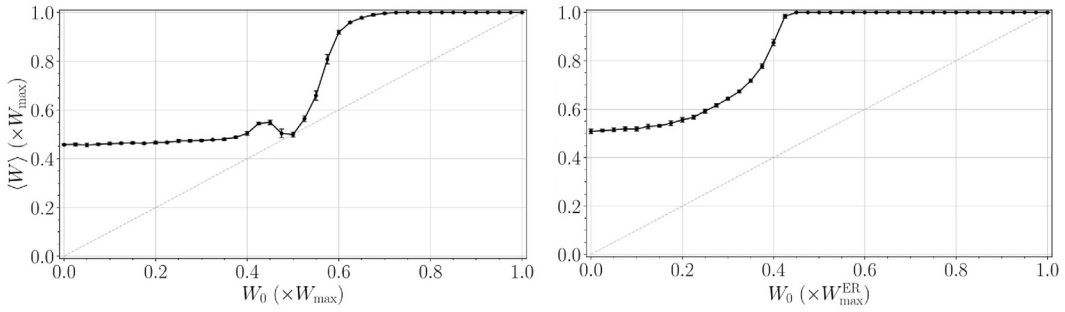

(a) $\epsilon = 0$ (b) $\epsilon = 0.032$

Fig. 3. Mean synaptic weight of the final state *vs* the initial synaptic weight value for the random network. The results are the average over 10 different initial conditions. The first bisector is also shown just for comparison. On panel (a) no noise is applied. In this case, for small W_0, the potentiation is caused by the coincidence of bursts of high-frequency neurons, while for large W_0, it is caused by the network's starting synchronisation. For intermediate W_0, there is a non-monotonic behaviour due to a segregation of the network in two clusters that operate in different frequencies. On panel (b) we show the same result but for simulations where noise is applied. The non-monotonic behaviour is not present in this case because there occurs no network segregation.

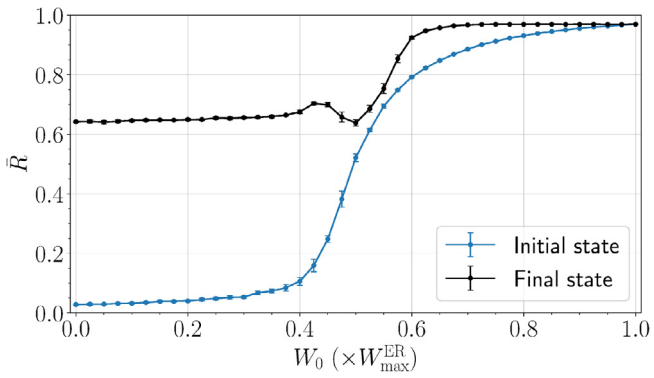

Fig. 4. Mean Kuramoto order parameter of the random network as a function of the initial synaptic weight value for before (blue line) and after (black line) plasticity's action for $\epsilon = 0$ (average on 10 initial conditions). (For interpretation of the references to colour in this figure legend, the reader is referred to the web version of this article.)

occurs for $W_0 \leqslant 0.45W_{\max}^{\mathrm{ER}}$ has a different origin than for $W_0 \geqslant 0.55W_{\max}^{\mathrm{ER}}$ due to the presence or not of an initial synchronisation.

We calculate the initial and final synchronisation of the noiseless random network by means of the Kuramoto order parameter. Fig. 4 displays the average of the Kuramoto order parameter over 10000 steps as a function of W_0 for before (blue line) and after (black line) the plasticity takes place. The curve of the initial state is the well known sigmoid-like curve of the order parameter *vs* coupling parameter. The curve for the asymptotic state is very similar to the one in Fig. 3(a), showing a correspondence between the average synaptic weight of the network with its synchronisation. The plasticity effect depends on the initial value of W_0. Due to this fact, we consider three different cases: $W_0 \leqslant 0.45W_{\max}^{\mathrm{ER}}$, $0.45W_{\max}^{\mathrm{ER}} < W_0 < 0.55W_{\max}^{\mathrm{ER}}$, and $W_0 \geqslant 0.55W_{\max}^{\mathrm{ER}}$.

For W_0 greater than about $0.55W_{\max}^{\mathrm{ER}}$, the order parameter of the initial state has values $\bar{R} \geqslant 0.7$, indicating the existence of burst synchronisation. This occurs due to the fact that the initial state synapses are strong enough to synchronise the network right from the start. After applying the plasticity rule, we observe for these W_0 an increase for $\langle W \rangle$ and $\bar{R}$. The increase of the mean synaptic weight is the result of the initial synchronisation, that causes the neurons to burst at almost the same time and thus potentiate the synapses. This mechanism of potentiation via synchronisation-caused burst coincidence is a Type I potentiation. As the synapses get stronger, the network becomes more synchronised, and as a consequence an increase on the order parameter is also observed. There is a positive feedback between synchronisation and potentiation, and this feedback is the reason that synaptic weights go to their maximum values. The synapses that connect synchronised neurons become stronger over time. In this case, we verify the formation of one synchronised cluster composed of all neurons of the network.

For W_0 smaller than $0.45W_{\max}^{\mathrm{ER}}$, the mean order parameter of the initial state has values $\bar{R} \leq 0.25$, indicating that the synchronisation in the initial state is low or inexistent. In this cases, the initial synapses are not strong enough to synchronise the neurons in the network. Applying the plasticity rule for small W_0 values, we also observe an increase in both $\langle W \rangle$ and $\bar{R}$, even without initial synchronisation. In particular, we identify synapse potentiation when $W_0 = W_{ij,t=0} = 0$, which is when there is no interaction between the neurons in the initial state. The potentiation comes not from synchronisation, but from a different phenomenon entirely, that is related to the natural neuronal frequencies. When there is no interaction between the neurons, the burst latency Δt assumes values randomly. Sometimes the value is small (and potentiation occurs) and other times it is large (and depression occurs). The maximum allowed value for Δt is the maximum inter-burst-interval (IBI) of the involved neurons. Neurons that exhibit high frequency (low IBI) have a narrower range of allowed values of Δt and, therefore, potentiation occurs more frequently than depression. This route to potentiation is called Type II potentiation. The minimum frequency for the potentiation is estimated to be $f_{\min} = 4.9 \times 10^{-3}$ (Appendix A), which is less than the frequency of many high-frequency neurons in the network. Once the synapses that connect the high-frequency neurons are strong enough, the neurons can become synchronised and kickstart the positive feedback between synchronisation and potentiation. They also start injecting current on other neurons in a united manner, and this joint action is enough to attract some medium-frequency neurons to the synchronised cluster.

Considering small values of W_0, we observe the formation of one cluster that is composed of the neurons with smaller inter-burst interval or higher firing burst frequency. The cluster formation is shown in Fig. 5, which represents the asymptotic value of the matrix **W** in a simulation for $W_0 = 0$ and no noise. In this figure, the pre and post synaptic index are sorted by increasing the natural burst frequency f_0. Blue (orange) dots correspond to the synapses with the maximal (minimal) weight values. We see that the neurons with higher burst frequency form a strongly connected cluster. We also note that the synaptic weight matrix becomes approximately symmetric along the main diagonal, meaning that the synapses between two neurons become stronger (or weaker) in both directions.

To make clearer the relation between potentiation and synchronisation for small values of W_0, we show in Fig. 6 the time evolution of the mean synaptic weight $\langle W \rangle$ of the order parameter R_t and its moving average $\mathrm{MA}(R_t)$ for $W_0 = 0$ and $\epsilon = 0$ until the asymptotic state to be reached. We verify that the potentiation begins before any synchronisation. At the start of the evolution ($t < 3 \times 10^5$), the mean synaptic weight slowly increases due to the coincidence of the high-frequency bursts. At this stage, the synchronisation does not increase, due to the fact that the connections among some neurons are not strong enough to synchronise them. At certain point ($t \approx 3 \times 10^5$), the synapses reach a critical strength level and synchronisation starts to arise. At this point, the positive feedback between the synchronisation and the potentiation is initiated, and as a consequence the synchronous behaviour increases more quickly. The synchronisation saturates when the synapses reach the maximum weight allowed.

Finally, for the intermediate values of W_0 ($0.45W_{\max}^{\mathrm{ER}} < W_0 < 0.55W_{\max}^{\mathrm{ER}}$), we identify the presence of both Type I and Type II mechanisms in the noiseless case. The order parameter values of the initial state are in the range $0.2 \leqslant \bar{R} \leqslant 0.7$, meaning that there is a partial synchronisation in the network. There are some neurons that are synchronised to each other and their synapses are potentiated. There are also some high-frequency neurons that do not start synchronised to the others. The synapses between these neurons are also strengthened due to the random coincidence of bursts. Then, there are two groups of synapses that are potentiated, where one is connected with synchronised neurons and the other that is connected with high-frequency neurons. However, the synapses connecting a high-frequency neuron to one that is part of the synchronised group are not potentiated, but instead they are depressed. For this reason, in this regime, we identify two separate clusters, one that is composed of neurons that potentiate via Type I mechanism and the other via Type II mechanism. We also find some neurons of low frequency that do not have any synapses that are potentiated at the

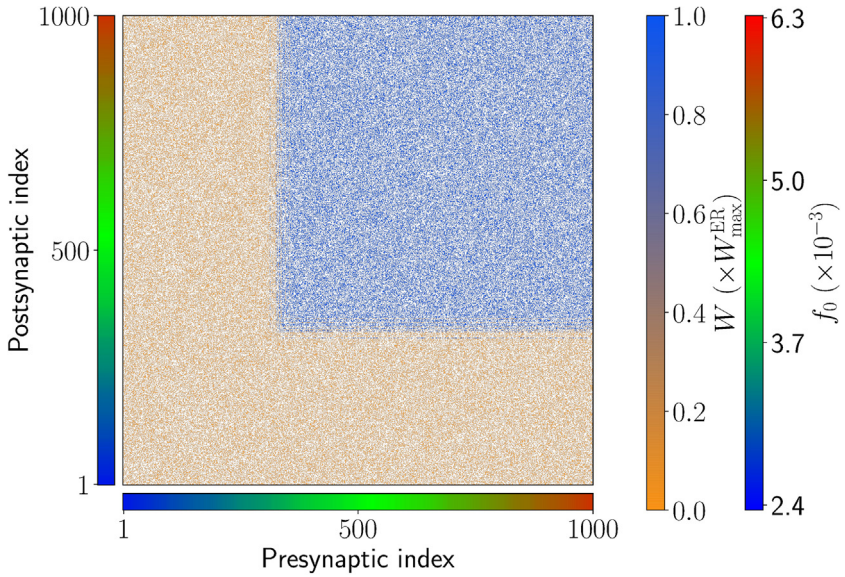

Fig. 5. Representation of the final state synaptic weight matrix **W** of the random network for $W_0 = 0$ and $\epsilon = 0$. Every synapse is denoted by a point, where the x-value is the index of the presynaptic neuron and the y-value is the postsynaptic index. Both axes are sorted by the neuron's natural mean frequency f_0 and the values are represented by the blue-green-red colourbars alongside the axes. The coloured points represent the values of the synaptic weights. The matrix **W** is approximately symmetric along the first diagonal. (For interpretation of the references to colour in this figure legend, the reader is referred to the web version of this article.)

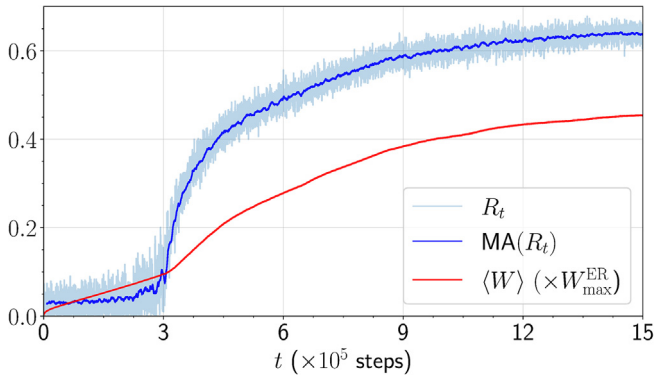

Fig. 6. Time series of the order parameter and the mean synaptic weight for the random network with $W_0 = 0$ and $\epsilon = 0$. The dark blue curve is the moving average MA(R_t) of the order parameter with window size of 8000 steps. (For interpretation of the references to colour in this figure legend, the reader is referred to the web version of this article.)

asymptotic state. These three groups of neurons are displayed in Fig. 7, which is similar to Fig. 5, but the initial weight is $W_0 = 0.5W^{\mathrm{ER}}_{\mathrm{max}}$ and we use the final mean frequency $\bar{f}_{\mathrm{end}}$ of the neuron to sort the axes. The two separated blue squares represent each one cluster. A consequence of the network division can be seen on Fig. 3(a) by the non-monotonic behaviour of the curve. As the initial synaptic weight increases from $0.45W^{\mathrm{ER}}_{\mathrm{max}}$ to $0.5W^{\mathrm{ER}}_{\mathrm{max}}$, one would expect the final average synaptic weight to increase as well. However, this does not occur, as in this range the group of highly connected neurons is broken into the two clusters. The synapses that connect one cluster to another (that would be potentiated were there only one single cluster) depress, and the average synaptic weight of the final state drops. The overall network synchronisation also suffers from the segregation, and the non-monotonic behaviour also appears in Fig. 4 on the asymptotic state curve of the order parameter.

In many cases — especially for lower values of W_0 — part of the neurons have all their synapses with synaptic weights close to zero on the asymptotic state, ending effectively cut-off from the network. These are the low-frequency neurons that present little synchronisation with the rest of the network at the start of the simulation. On the other hand, connections that remain on the asymptotic state have maximum weight value. It can be said, therefore, that the BTDP rule by itself has a extremizing effect, by which neurons that have little correlation are driven further apart, and correlated neuron are driven closer together. This is consistent with the hebbian nature of the plasticity rule.

We identified two possible mechanisms for potentiation in the random network, whose occurrence depends on the value of starting synaptic weights. We now analyse the reason these mechanisms are only present for some W_0 values. In the top row of Fig. 8, we plot the initial mean frequency as a function of the neuron's natural frequency for three values of W_0, one for each regime. For $W_0 \leqslant 0.45W^{\mathrm{ER}}_{\mathrm{max}}$, the neuron's mean frequency before plasticity actuated is approximately equal its mean natural frequency. As an example, Fig. 8(a) depicts the case where $W_0 = 0$. In this situation, the potentiation mechanism is due to the low IBI random burst coincidence (Type II), Because there are neurons that exhibit high frequency and no initial synchronisation. For $W_0 \geqslant 0.55W^{\mathrm{ER}}_{\mathrm{max}}$, the network is initially synchronised and the neurons's frequencies are altered. The plateau in Fig. 8(c) shows that for $W_0 = 0.7W^{\mathrm{ER}}_{\mathrm{max}}$ most neurons exhibit the same common frequency. This common frequency is not high enough for the Type II mechanism to occur and, therefore, only the Type I potentiation is present. On the other hand, for intermediate W_0, the initial synchronisation does not encompasses all neurons. In Fig. 8(b) we see a plateau of synchronised neurons and also the existence of neurons whose frequency is not completely altered to the common one. As there exists neurons that are synchronised, as well as neurons that exhibit high frequency, we observe both Type I and Type II potentiation mechanisms. However, the same neuron is only affected mainly by one of the two types.

The final state of the neurons's frequency was also computed and is depicted on the bottom row of Fig. 8. The colours indicate the cluster to which the neurons belongs. We consider red for the Type I cluster, blue for the Type II, and yellow for low frequency neurons whose synapses do not potentiate. The same colours are kept in the top row for comparison's sake. The plateau regions in

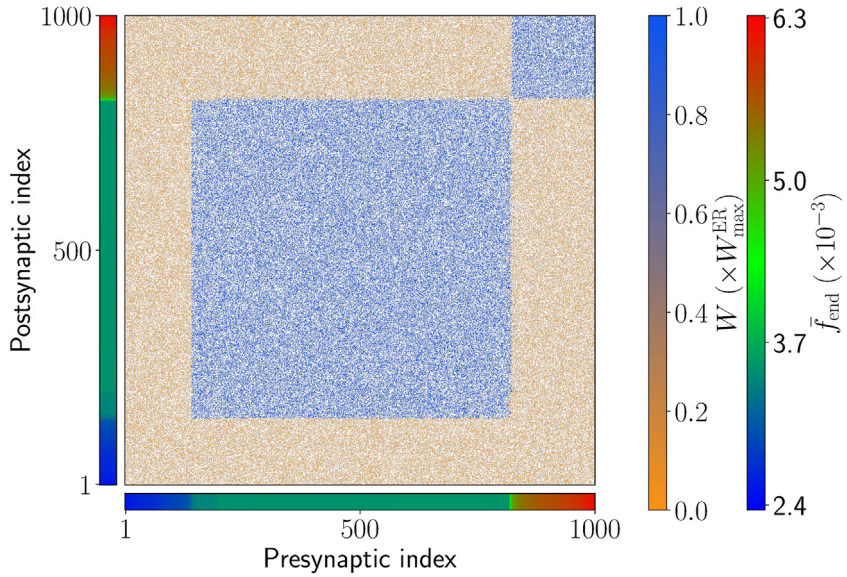

Fig. 7. Final state synaptic weight matrix **W** of the random network for $W_0 = 0.5W^{ER}_{max}$ and $\epsilon = 0$ (see Fig. 5 for explanation). The axes are sorted by the neuron's final mean frequency. The neurons initially synchronised have the synapses potentiated by the Type I mechanism and form a cluster (big blue square in the middle). On the other hand, synapses that are connected with high-frequency neurons are potentiated by the Type II mechanism (smaller square on the top right corner). The synapses that are connected with high-frequency and initially frequency-locked neurons are depressed. (For interpretation of the references to colour in this figure legend, the reader is referred to the web version of this article.)

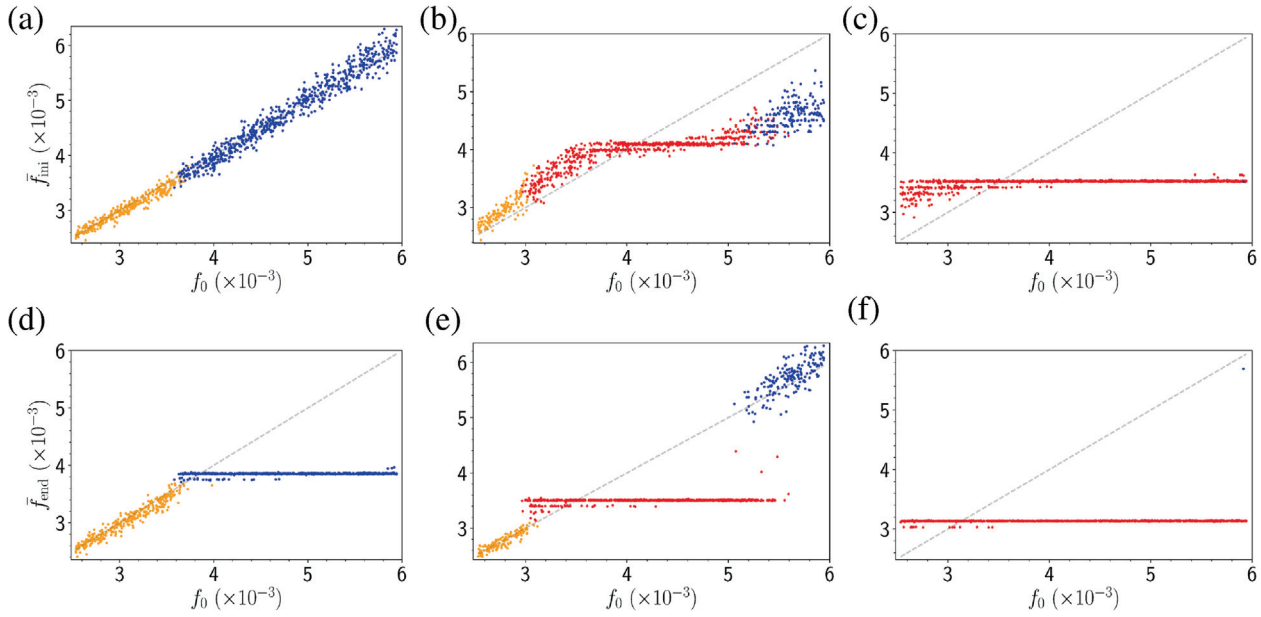

Fig. 8. $\bar{f}_{ini} \times f_0$ for (a) $W_0 = 0$, (b) $W = 0.5W^{ER}_{max}$, and (c) $W = 0.7W^{ER}_{max}$, and $\bar{f}_{end} \times f_0$ for (d) $W_0 = 0$, (e) $W = 0.5W^{ER}_{max}$, and (f) $W = 0.7W^{ER}_{max}$. Results for the random network with no noise. The colour indicates which cluster a neuron belongs, where red is the Type I cluster, blue for the Type II cluster, and yellow for low frequency neurons that do not belong to any cluster. The plateaus indicate frequency-synchronised neurons. (For interpretation of the references to colour in this figure legend, the reader is referred to the web version of this article.)

these figures exhibit the presence of frequency synchronisation in the final state. We note that for small values of W_0, Type II potentiation leads to a synchronised cluster (Fig. 8(d)), while for intermediate W_0 values, the same potentiation mechanism leads to a desynchronised cluster (Fig. 8(e)). For $W_0 = 0.5W^{ER}_{max}$, this cluster exhibits a local order parameter of 0.213, meaning that the neurons are not very synchronised. On the other hand, clusters that are created by the Type I mechanism have synchronised neurons. The local order parameter for this cluster for $W_0 = 0.5W^{ER}_{max}$ has value 0.909.

Next we consider the addition of noise on the network and the robustness of the results is analysed. We use a gaussian-distributed noise with mean zero, unitary standard deviation and amplitude ϵ. The noise is applied to all neurons independently. When the noise amplitude is low, the effects of the plasticity are not altered, and cluster segregation is stil present. However, for noise levels as high as $\epsilon = 0.032$, the behaviour changes. The final average synaptic weight for this case is shown in Fig. 3(b) as a function of W_0. We observe that the non-monotonic behaviour present in the noiseless network no longer appears with the addi-

tion of noise. The transition is instead smooth. The absence of the non-monotonic behaviour is also observed on the order parameter curve. The segregation of the network in clusters is also absent.

It was observed that, for when the initial synchronisation level is low, the noise has the effect of increasing the initial burst frequency of the neurons when compared to the noiseless network. Fig. 9 depicts the neurons's frequency on the initial state for $W_0 = 0.5W^{ER}_{max}$ and $\epsilon = 0.032$. When compared to its noiseless counterpart in Fig 8(b), we see that the addition of noise increases the neurons's burst frequency and diffuses the initial frequency synchronisation. As a result the distinction between Type I and Type II potentiation becomes blurred, and segregation is made more difficult. The image representation of the final synaptic weight matrix (not shown) is similar to the one on Fig. 5 for the whole W_0 parameter space. The size of the blue square increases with W_0 until it encompasses the whole network on $W_0 \sim 0.45W^{ER}_{max}$. Thus, only one cluster is found on the network if high amplitude noise is present.

3.2. Small-world network

We now analyse the effect of BTDP on the small-world network. We consider the dynamics of the network without noise ($\epsilon = 0$). At the start of the simulation we set the synaptic weights of all synapses to the same value W_0. Simulations were made with W_0 ranging from 0 to W^{WS}_{max}. It was observed that for small values of starting synaptic weight ($W_0 < 0.3W^{WS}_{max}$) local synapses are heavily favoured to potentiate over non-local synapses. By non-local synapses we mean the shortcuts of the Watts-Strogatz method. In this range, very few non-local synapses were potentiated, most were depressed to vanishing synaptic weight. This means the network exhibited essentially a local characteristic in this interval. From $W_0 = 0$ through $W_0 = 0.275W^{WS}_{max}$ the fraction of potentiated local synapses steadily increases from 49% to 97%, while the fraction of potentiated non-local synapses only increases from 10% to 15% in this range. However, when W_0 assumes the value $0.3W^{WS}_{max}$, a large portion of the non-local synapses potentiate together. For initial synaptic weight values greater or equal to $0.3W^{WS}_{max}$, the network is not predominantly local as it is for lower W_0 values, but becomes non-local with small-world properties.

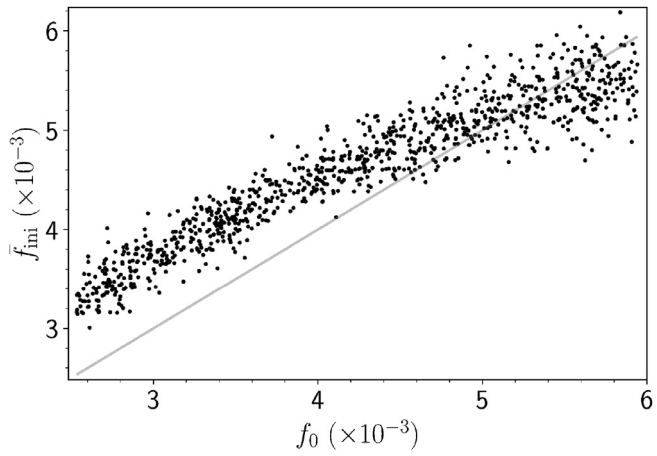

Fig. 9. Frequency of the neurons before plasticity action for a random network with $W_0 = 0.5W^{ER}_{max}$ and noise of amplitude $\epsilon = 0.032$. With the addition of noise, the initial frequency of the neurons is increased, and the frequency locking is weakened when compared to the noiseless case, depicted in Fig. 8(b). Because of that, the segregation of the network in clusters does not occur.

This transition can be seen in Figs. 10 and 11, that show the synaptic weight matrix **W** on the final state of simulations for two values of W_0. The position of the points is the same as in the adjacency matrix, and the colours represent the final synaptic weight value of the synapses. It is clear that for $W_0 = 0.275W^{WS}_{max}$ the density of potentiated synapses, represented by blue points, is much larger for local synapses (near the diagonal) than for non-local synapses. But for $W_0 = 0.3W^{WS}_{max}$ a large part of non-local synapses got potentiated.

The global behaviour of this transition is shown in Figs. 12 and 13, that depict the final average synaptic weight and the mean order parameter, respectively, as a function of W_0. For $W_0 < 0.3W^{WS}_{max}$ the main non-zero contribution to $\langle W \rangle$ comes from the local synapses. But when W_0 reaches $0.3W^{WS}_{max}$ the non-local synapses start contributing as well, and a quick increase is seen in the average synaptic weight. The transition is even more noticeable on the final state order parameter. Because the order parameter is a measure of global synchrony, it does not capture well the local synchronisation present on the network for $W_0 < 0.3W^{WS}_{max}$, and so it assumes very low values in this range. Once the non-local connections become relevant, global synchronisation arises, and so the order parameter immediately increases in

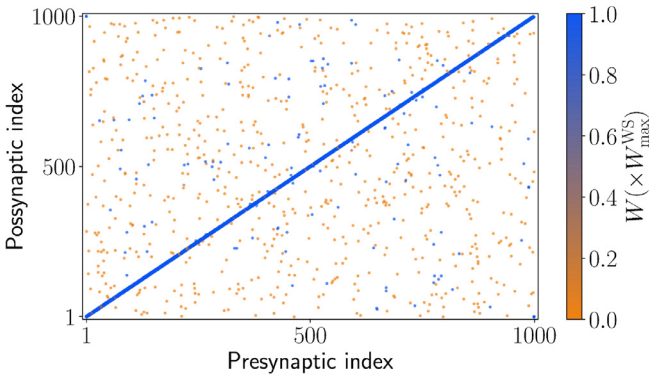

Fig. 10. Synaptic weight matrix of the small-world network on the asymptotic state in a simulation where $W_0 = 0.275W^{WS}_{max}$. Blue points represent potentiated synapses, and orange points depressed synapses. For initial synaptic weights smaller or equal to $0.275W^{WS}_{max}$, the great majority of potentiated synapses are local ones, close to the diagonal of the adjacency matrix. The potentiated non-local synapses are few and the network exhibits essentially local properties. (For interpretation of the references to colour in this figure legend, the reader is referred to the web version of this article.)

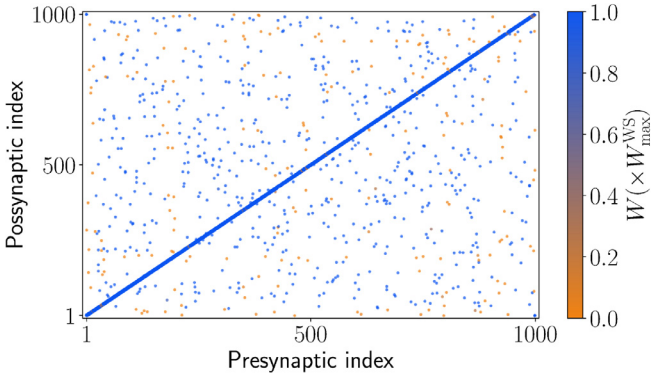

Fig. 11. Synaptic weight matrix of the small-world network on the asymptotic state in a simulation where $W_0 = 0.3W^{WS}_{max}$. As opposed to lower values of W_0, a large part of the non-local synapses become potentiated, and the network exhibits non-local properties.

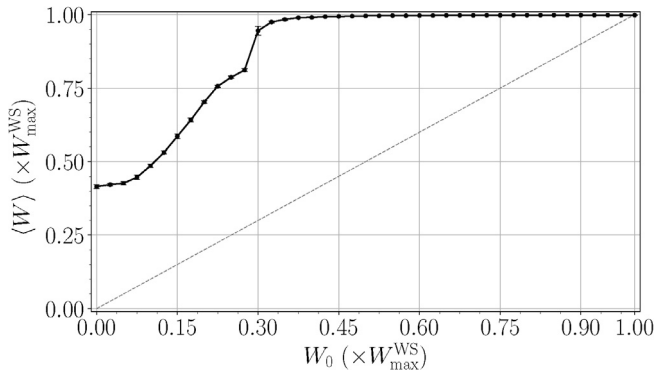

Fig. 12. Average synaptic weight on the final state as a function of the initial synaptic weight for the small-world network (average in 10 initial conditions). The plasticity rule increases the average connection strength of the network for all tested values of W_0. For $W_0 < 0.3W_{\max}^{WS}$, the majority of non-zero contribution to $\langle W \rangle$ comes from local synapses. The fraction of potentiated local synapses increases in this range. After $W_0 = 0.3W_{\max}^{WS}$, practically all synapses get potentiated.

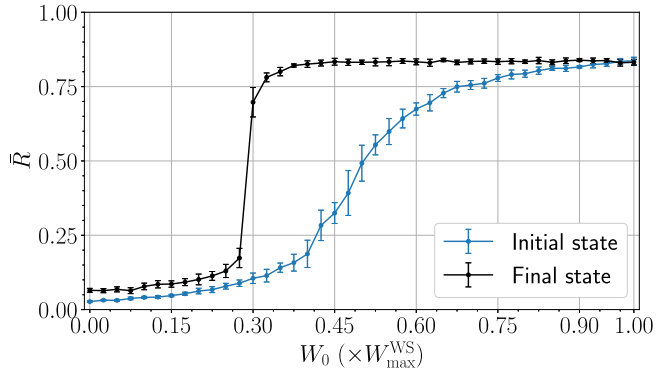

Fig. 13. Mean order parameter on the initial and asymptotic state for the small-world network as a function of the initial synaptic weight (average in 10 initial conditions). For $W_0 < 0.3W_{\max}^{WS}$, the network exhibits local properties, and the order parameter does not capture global synchronisation. However, when the non-local synapses get potentiated starting in $W_0 = 0.3W_{\max}^{WS}$, the synchronisation degree of the network immediately rises.

value. As the synaptic weight of potentiated synapses is maximum, the level of synchronisation when the non-local synapses are present is very high.

It should also be noted that, as opposed to the random network, there is no separation of the network in two clusters. In the case of the random network, the neuron bursting frequency is the primary factor to determine synapse potentiation, because the number of synapses each neuron has is high and the distribution of synapses is homogeneous. Because of this, a clear separation of frequency could result in a clear separation in clusters. But in the small-world case, the adjacency matrix also plays an important role in determining which synapses potentiate, because neurons have a limited group of available synapses. As a result, network segregation is not as easy to occur for the small-world network.

4. Conclusions

In this work we study how burst-time dependent plasticity (BTDP) affects a random network and a small-world network composed of Rulkov neurons connected by excitatory chemical synapses. We calculate the mean synaptic weight, individual burst frequency, and synchronisation level of the neurons.

For the random network, we consider low, medium, and high initial synchronous activity. In this framework, we observe two different mechanisms of synaptic potentiation which are associated with the BTDP rule. The first is related to a high initial synchronisation of the network (Type I), and the second to a statistical properties of high-frequency neurons (Type II). In the transition between this two regimes, we verify mixed regimes with the presence of both mechanisms. Depending on the initial synaptic weights, we identify the formation of one or two clusters. When only one mechanism is present, it generates a synchronised cluster. For two clusters, we show that one cluster has desynchronised neurons with high burst frequency, while the other is generated by the Type I mechanism and exhibits neurons with synchronised activity. The segregation in two clusters does not occur if a gaussian noise with high enough amplitude is added to the network. Both in the absence or presence of noise the plasticity can create a strongly connected nucleus with a subset of the network neurons, while leaving the other neurons isolated from the network.

For the small-world network, the final state exhibits local characteristics when the initial synaptic weight value is low. Increasing the initial synaptic weight, there is a transition in which a large part of the non-local synapses become potentiated, and the network loses the local aspect. As opposed to the random network, the structure of the adjacency matrix plays a key role in determining which synapses get potentiated for the small-world network.

CRediT authorship contribution statement

João Antonio Paludo Silveira: Conceptualization, Methodology, Software, Data curation, Writing - original draft, Writing - review & editing, Visualization, Investigation, Validation. **Paulo Ricardo Protachevicz:** Conceptualization, Methodology, Validation, Writing - review & editing. **Ricardo Luiz Viana:** Conceptualization, Methodology, Validation, Writing - review & editing. **Antonio Marcos Batista:** Conceptualization, Methodology, Validation, Writing - review & editing, Supervision.

Declaration of Competing Interest

The authors declare that they have no known competing financial interests or personal relationships that could have appeared to influence the work reported in this paper.

Acknowledgements

This work was possible by partial financial support from the following Brazilian government agencies: CNPq, CAPES, FAPESP (2020/04624-2), and Fundação Araucária. We would like to thank www.105groupscience.com.

Appendix A. Minimum frequency for potentiation via random coincidence

Consider the simple model of two neurons with constant bursting frequency f_1 and f_2. We ask that $0.5 \lesssim f_1/f_2 \lesssim 2$ — so that a burst from a neuron is mostly followed by a burst of the other neuron — and that this ratio be an irrational number. We suppose that there is no coupling between the neurons and the inter-burst-intervals are constant with values $\mathrm{IBI}_1 = 1/f_1$ and $\mathrm{IBI}_2 = 1/f_2$.

Then, the burst latency Δt will never take on the same value twice and, if we ignore events where one neuron fires twice before the other, will have for large times visited all regions of the allowed interval uniformly. So as time tends to infinity the burst-latency probability distribution approaches a uniform distribution on the allowed values.

$$\mathscr{P}(\Delta t) = \begin{cases} 1/\Delta t_{\max} & 0 < \Delta t < \Delta t_{\max} \\ 0 & \text{otherwise} \end{cases} \quad (A.1)$$

where $\Delta t_{\max}$ is the maximum possible burst-latency value. The way the plasticity rule was implemented in our simulation this value is $\Delta t_{\max} = \max(\text{IBI}_1, \text{IBI}_2)$. The average long-term synaptic weight change of a synapse between these two neurons can then be calculated by

$$\begin{aligned} \overline{\Delta W} &= \int_0^{\infty} \Delta W(t)\mathscr{P}(t)\mathrm{d}t \\ &= \frac{1}{\Delta t_{\max}}\left\{\int_0^{T_s}\left(P - \frac{P-D}{T_s}t\right)\mathrm{d}t + \int_{T_s}^{\Delta t_{\max}} D\mathrm{d}t\right\}, \end{aligned} \quad (A.2)$$

where Eq. 3 was used with the implementation values $A_p \to P$, $A_d \to D$. We also assumed that $\Delta t_{\max} > T_s$. We then get

$$\overline{\Delta W} = D + \frac{P-D}{2}\frac{T_s}{\Delta t_{\max}}. \quad (A.3)$$

To obtain the condition for potentiation at large times we ask that $\overline{\Delta W} > 0$, which results in

$$\frac{\Delta t_{\max}}{T_s} < 1 - \frac{A_p}{A_d}. \quad (A.4)$$

Here, we have already exchanged the computer implementation values for the BTDP function ones: $D = A_d/2, P = A_p - D$. Plugging in the numeric values used on the simulation, we get that potentiation occurs when

$$\max(\text{IBI}_1, \text{IBI}_2) < 203, \quad (A.5)$$

or equivalently

$$\min(f_1, f_2) > 4.93 \times 10^{-3}. \quad (A.6)$$

One would then expected, that the synapse of two uncoupled neurons with mean frequency f_1 and f_2, which satisfy the condition A.6 will get potentiated for large times.

References

[1] A.W. Toga, P.M. Thompson, Mapping brain asymmetry, Nat. Rev. Neurosci. 4 (2003) 37–48.
[2] J. DeFelipe, P. Marco, I. Busturia, A. Merchán-Pérez, Estimation of the number of synapses in the cerebral cortex: methodological considerations, Cereb. Cortex 9 (1999) 722–732.
[3] S. Ciocchi, J. Passecker, H. Malagon-Vina, N. Mikus, T. Klausberger, Selective information routing by ventral hippocampal CA1 projection neurons, Science 348 (2015) 560–563.
[4] A.E. Pereda, Electrical synapses and their functional interactions with chemical synapses, Nat. Rev. Neurosci. 15 (2014) 250–263.
[5] P. Mateos-Aparicio, A. Rodríguez-Moreno, The impact of studying brain plasticity, Front. Cell. Neurosci. 13 (2019) 66.
[6] W. James, The Principles of Psychology, Harvard University Press, Cambridge, 1890.
[7] J. DeFelipe, Brain plasticity and mental processes: cajal again, Nat. Rev. Neurosci. 7 (2006) 811–817.
[8] K.S. Lashley, The behavioristic interpretation of consciousness I, Psychol. Rev. 30 (1923) 237–272.
[9] D.O. Hebb, The Organization of Behavior; A Neuropsychological Theory, Wiley, New York, 1949.
[10] T. Lomo, The discovery of long-term potentiation, Philos. Trans. R. Soc. Lond. B Biol. Sci. 358 (2003) 617–620.
[11] E.L. Lameu, E.E.N. Macau, F.S. Borges, K.C. Iarosz, I.L. Caldas, R.R. Borges, P. Prottachevicz, R.L. Viana, A.M. Batista, Alterations in brain connectivity due to plasticity and synaptic delay, Eur. Phys. J. Spec. Top. 227 (2018) 673–682.
[12] O.V. Popovych, S. Yanchuk, P.A. Tass, Self-organized noise resistance of oscillatory neural networks with spike timing-dependent plasticity, Sci. Rep. 3 (2013) 2926.
[13] R.R. Borges, F.S. Borges, E.L. Lameu, A.M. Batista, K.C. Iarosz, I.L. Caldas, C.G. Antonopoulos, M.S. Baptista, Spike timing-dependent plasticity induces non-trivial topology in the brain, Neural Netw. 88 (2017) 58–64.
[14] R.R. Borges, F.S. Borges, E.L. Lameu, P. Prottachevicz, K.C. Iarosz, I.L. Caldas, R.L. Viana, E.E.N. Macau, M.S. Baptista, C. Grebogi, A.M. Batista, Synaptic plasticity and spike synchronisation in neuronal networks, Braz. J. Phys. 47 (2017) 678–688.
[15] R.R. Borges, F.S. Borges, E.L. Lameu, A.M. Batista, K.C. Iarosz, I.L. Caldas, R.L. Viana, M.A.F. Sanjuán, Effects of the spike timing-dependent plasticity on the synchronisation in a random Hodgkin-Huxley neuronal network, Commun. Nonlinear Sci. Numer. Simul. 34 (2016) 12–22.
[16] D.A. Butts, P.O. Kanold, C.J. Shatz, A burst-based "Hebbian" learning rule at retinogeniculate synapses links retinal waves to activity-dependent refinement, PLoS Biol. 5 (2007) e61.
[17] Y. Kuramoto, Chemical Oscillations, Waves, and Turbulence, Springer-Verlag, Berlin, 1984.
[18] Z. Wang, S. Baruni, F. Parastesh, S. Jafari, D. Ghosh, M. Perc, I. Hussain, Chimera in an adaptive neuronal network with burst-timing-dependent plasticity, Neurocomputing 406 (2020) 117–126, doi: 10.1016/j.neucom.2020.03.083.
[19] Z. Yao, X. Yang, Z. Sun, How synaptic plasticity influences spike synchronisation and its transitions in complex neural network, Chaos 28 (2018) 083120.
[20] G. Deco, A. Buehlmann, T. Masquelier, E. Hugues, The role of rhythmic neural synchronisation in rest and task conditions, Front. Hum. Neurosci. 5 (2011) 4.
[21] J. Jiang, B. Dai, D. Peng, C. Zhu, L. Liu, C. Lu, Neural synchronisation during face-to-face communication, J. Neurosci. 32 (2012) 16064–16069.
[22] P.U. Uhlhaas, W. Singer, Neural synchrony in brain disorders: relevance for cognitive dysfunctions and pathophysiology, Neuron 52 (2006) 155–168.
[23] L.L. Rubchinsky, C. Park, R.M. Worth, Intermittent neural synchronisation in Parkinson's disease, Nonlinear Dyn. 68 (2012) 329–346.
[24] C. Babiloni, C. Del Percio, R. Lizio, G. Noce, S. Cordone, S. Lopez, A. Soricelli, R. Ferri, M.T. Pascarelli, F. Nobili, D. Arnaldi, F. Famà, D. Aarsland, F. Orzi, C. Buttinelli, F. Giubilei, M. Onofrj, F. Stocchi, P. Stirpe, P. Fuhr, U. Gschwandtner, G. Ransmayr, G. Caravias, H. garn, F. Sorpresi, M. Pievani, F. D'Antonio, C. De Lena, B. Güntekin, L. Hanoglu, E. Basar, G. Yener, D.D. Emek-Savas, A.I. Triggiani, R. Franciotti, G.B. Frisoni, L. Banonni, M.F. De Pandis, Abnormalities of cortical neural synchronisation mechanisms in subjects with mild cognitive impairment due to Alzheimer's and Parkinson's diseases: an EEG study, J. Alzheimers Dis. 59 (2017) 339-359..
[25] O. Devinsky, A. Vezzani, T.J. O'Brien, N. Jette, I.E. Scheffer, M. de Curtis, P. Perucca, Epilepsy, Nat. Rev. 3 (2018) 18024.
[26] C.A.S. Batista, E.L. Lameu, A.M. Batista, S.R. Lopes, T. Pereira, G. Zamora-López, J. Kurths, R.L. Viana, Phase synchronisation of bursting neurons in clustered small-world networks, Phys. Rev. 85 (2012) 016211.
[27] N.F. Rulkov, Regularization of synchronised chaotic bursts, Phys. Rev. Lett. 86 (2001) 183–186.
[28] P. Erdös, A. Rényi, On random graphs, Publ. Math. Debrecen 6 (1959) 290–297.
[29] X. Shi, X. Sun, Y. Lv, Q. Lu, H. Wang, Cluster synchronisation and rhythms dynamics in a complex neuronal network with chemical synapses, Int. J. Nonlinear Mech. 70 (2015) 112–118.
[30] D.J. Watts, S.H. Strogatz, Collective dynamics of 'small-world' networks, Nature 393 (1998) 440–442.
[31] D.S. Bassett, E. Bullmore, Small-world brain networks, Neuroscientist 12 (2006) 512–523.

João Antonio Paludo Silveira is 23 years old and lives in Curitiba – Brazil. He holds a bachelor degree in physics from the Federal University of Paraná, and is currently (2020) pursuing a master's degree at the same university. His main focus of study is synchronization and plasticity on neuronal networks.

Paulo Ricardo Protachevicz received the B.S. degree in Physics (2013), M.S. (2016) and Ph.D. (2020) degrees in Science/Physics from State University of Ponta Grossa, Paraná, Brazil. He is currently a post-doctoral research fellow at Institute of Physics of University of São Paulo. His research interests include plasticity, neuronal dynamics and synchronization.

Ricardo Luiz Viana is a Full Professor in the Physics Department of the Federal University of Paraná, and works there since 1989. He has a D.Sc. in Plasma Physics (São Paulo University, 1991) and completed post-doctoral in the University of Maryland at College Park (1997) on Nonlinear Dynamics. He is the founder and currently the head of the Plasma Physics and Nonlinear Dynamics Group. His main research subjects are in applied nonlinear dynamics, including computational neuroscience.

Antonio Marcos Batista is a Bachelor in Physics at the State University of Ponta Grossa (1994), Master of Science at the Federal University of Paraná (1996), PhD in Physics at the Federal University of Paraná (2001), Postdoc in Physics at the University of São Paulo (2004–2006), and Postdoc in Biophysics at Institute for Complex Systems and Mathematical Biology in University of Aberdeen UK (2013–2014). He has experience in Physics, acting on the following subjects: networks, plasma, and biophysics.